

Search for thj production with $h \rightarrow \gamma\gamma$ at the LHC in the littlest Higgs model with T-parity

Bingfang Yang,^{*} Biaofeng Hou, and Huaying Zhang

¹ *College of Physics and Materials Science,
Henan Normal University, Xinxiang 453007, China*

(Dated: November 7, 2018)

Abstract

In the littlest Higgs model with T-parity, we study associated production of a Higgs and a single top quark at the 14 TeV LHC. We focus on the Higgs to two photons decay and the semileptonic top decay channel. By performing a fast detector simulation, we find that the thj search in the selected channel can excluded the top partner mass m_{T_+} up to 805 (857) GeV for case A (case B) at 2σ confidence level at 14 TeV LHC with the integrated luminosity $L = 3\text{ab}^{-1}$.

PACS numbers: 14.65.Ha, 14.80.Ly, 11.30.Hv

^{*}Electronic address: yangbingfang@htu.edu.cn

I. INTRODUCTION

The discovery of a Higgs boson with the CMS and ATLAS experiments in 2012 [1] opened a new field for explorations in the realm of particle physics. In order to test whether the Higgs boson is the one predicted by the Standard Model (SM), it is critical to explore the coupling of this Higgs boson with the other elementary particles. In particular, the Yukawa coupling of the Higgs to fermions is an important class, where the top quark owns the strongest Yukawa coupling due to the large mass. So, it is widely believed that the top quark is sensitive to the electroweak symmetry breaking mechanism and new physics[2].

As a direct probe of the top Yukawa coupling, the Higgs boson production in association with top-quark pair is a golden channel. But, it is only sensitive to the magnitude of the top Yukawa coupling rather than its sign. As a beneficial supplement, the production of a Higgs boson in association with single top quark can bring a unique possibility[3]. Higgs boson plus single top quark production proceeds through three modes, that is t -channel($pp \rightarrow thj$), s -channel($pp \rightarrow th\bar{b}$) and W -associated production ($pp \rightarrow thW$), where the t -channel is the dominant mode. Recently, this process has been measured by the CMS experiments[4]. Meanwhile, the relevant phenomenological studies have been carried out extensively[5].

The littlest Higgs model with T-parity (LHT)[6] was proposed as a possible solution to the hierarchy problem and so far remains a popular candidate of new physics. The LHT model predicts new gauge bosons, scalars and top partner, they are responsible for canceling the quadratic divergence contribution to Higgs boson mass from the SM gauge boson loops, Higgs self-energy and top quark loop, respectively. These new particles may contribute to the $pp \rightarrow thj$ process. Besides, the Higgs couplings are modified with respect to their SM values and this effect can also influence the process $pp \rightarrow thj$. By performing the detailed analysis on the process $pp \rightarrow thj$ may provide a good opportunity to probe the LHT signal, and the Higgs to $b\bar{b}$ decay channel has been studied in our previous work[7]. In this paper, we will focus on this process and investigate the observability of $pp \rightarrow thj$ with the semileptonic decay of the top quark and the diphoton decay of the Higgs boson. Though the diphoton branching fraction of the Higgs boson is very small, the diphoton final state allows very good background rejection thanks to the excellent diphoton invariant mass resolution provided by the CMS detector.

The paper is organized as follows. In Sec.II we give a brief review of the LHT model

related to our work. In Sec.III we explore the observability of the process $pp \rightarrow thj$ with $t \rightarrow \ell^+ \nu b$ and $h \rightarrow \gamma\gamma$ at 14 TeV LHC by performing a fast detector simulation and make some discussions. Finally, we give a summary in Sec.IV.

II. A BRIEF REVIEW OF THE LHT MODEL

The LHT model was based on a non-linear σ model describing an $SU(5)/SO(5)$ symmetry breaking, with the global group $SU(5)$ being spontaneously broken into $SO(5)$ by a 5×5 symmetric tensor at the scale $f \sim \mathcal{O}(\text{TeV})$.

In the fermion sector, the implementation of T -parity requires the existence of mirror partners for each original fermion. In order to do this, two fermion $SU(2)$ doublets q_1 and q_2 are introduced and T -parity interchanges these two doublets. A T -even combination of these doublets is taken as the SM fermion doublet and the T -odd combination is its T -parity partner. The doublets q_1 and q_2 are embedded into incomplete $SU(5)$ multiplets Ψ_1 and Ψ_2 as $\Psi_1 = (q_1, 0, 0_{1 \times 2})^T$ and $\Psi_2 = (0_{1 \times 2}, 0, q_2)^T$. To give the additional fermions masses, an $SO(5)$ multiplet Ψ_c is also introduced as $\Psi_c = (q_c, \chi_c, \tilde{q}_c)^T$, where χ_c is a singlet and q_c is a doublet under $SU(2)$. Their transformation under the $SU(5)$ is non-linear: $\Psi_c \rightarrow U\Psi_c$, where U is the unbroken $SO(5)$ rotation in a non-linear representation of the $SU(5)$. The components of the latter Ψ_c multiplet are the so-called mirror fermions. Then, one can write down the following Yukawa-type interaction to give masses of the mirror fermions

$$\mathcal{L}_{\text{mirror}} = -\kappa_{ij} f (\bar{\Psi}_2^i \xi + \bar{\Psi}_1^i \Sigma_0 \Omega \xi^\dagger \Omega) \Psi_c^j + h.c. \quad (1)$$

where $\Omega = \text{diag}(1, 1, -1, 1, 1)$, $i, j = 1, 2, 3$ are the generation indices. The masses of the mirror quarks u_H^i, d_H^i and mirror leptons l_H^i, ν_H^i up to $\mathcal{O}(v^2/f^2)$ are given by

$$m_{d_H^i} = \sqrt{2}\kappa_i f, \quad m_{u_H^i} = m_{d_H^i} \left(1 - \frac{v^2}{8f^2}\right), \quad (2)$$

$$m_{l_H^i} = \sqrt{2}\kappa_i f, \quad m_{\nu_H^i} = m_{l_H^i} \left(1 - \frac{v^2}{8f^2}\right), \quad (3)$$

where κ_i are the diagonalized Yukawa couplings, $v = v_{SM}(1 + \frac{1}{12} \frac{v_{SM}^2}{f^2})$ and $v_{SM} = 246$ GeV is the vacuum expectation value of the SM Higgs field.

In the top quark sector, two singlet fields T_{L_1} and T_{L_2} (and their right-handed counterparts) are introduced to cancel the large radiative correction to the Higgs mass induced by the top quark. Both fields are embedded together with the q_1 and q_2 doublets into the $SU(5)$

multiplets: $\Psi_{1,t} = (q_1, T_{L_1}, 0_2)^T$ and $\Psi_{2,t} = (0_2, T_{L_2}, q_2)^T$. The T -even combination of q_i is the SM fermion doublet and the other T -odd combination is its T -parity partner. Then, the T -parity invariant Yukawa Lagrangian for the top sector can be written down as follow:

$$\begin{aligned} \mathcal{L}_t = & -\frac{\lambda_1 f}{2\sqrt{2}} \epsilon_{ijk} \epsilon_{xy} \left[(\bar{\Psi}_{1,t})_i \Sigma_{jx} \Sigma_{ky} - (\bar{\Psi}_{2,t} \Sigma_0)_i \Sigma'_{jx} \Sigma'_{ky} \right] t'_R \\ & -\lambda_2 f (\bar{T}_{L_1} T_{R_1} + \bar{T}_{L_2} T_{R_2}) + \text{h.c.} \end{aligned} \quad (4)$$

where ϵ_{ijk} and ϵ_{xy} are the antisymmetric tensors with $i, j, k = 1, 2, 3$ and $x, y = 4, 5$, $\Sigma' = \langle \Sigma \rangle \Omega \Sigma^\dagger \Omega \langle \Sigma \rangle$ is the image of Σ under T -parity, λ_1 and λ_2 are two dimensionless top quark Yukawa couplings, t'_R and $T_{R_m} (m = 1, 2)$ are $SU(2)$ singlets. Under T -parity, these fields transform as: $T_{L_1} \leftrightarrow -T_{L_2}$, $T_{R_1} \leftrightarrow -T_{R_2}$, $t'_R \rightarrow t'_R$. So, the T -parity eigenstates can be defined as

$$t_{L+} = (t_{L_1} - t_{R_1})/\sqrt{2}, \quad T'_{L\pm} = (T_{L_1} \mp T_{L_2})/\sqrt{2}, \quad T'_{R\pm} = (T_{R_1} \mp T_{R_2})/\sqrt{2}. \quad (5)$$

At the tree level, the T'_{L-} and T'_{R-} do not mix with the mirror fermions and the T-odd Dirac fermion $T_- = (T'_{L-}, T'_{R-})$ does not interact with Higgs boson. However, the two T-even eigenstates (t_{L+}, t'_R) and (T'_{L+}, T'_{R+}) mix with each other so that the mass eigenstates can be defined as

$$\begin{aligned} t_L &= \cos \beta t_{L+} - \sin \beta T'_{L+}, & T_{L+} &= \sin \beta t_{L+} + \cos \beta T'_{L+}, \\ t_R &= \cos \alpha t'_R - \sin \alpha T'_{R+}, & T_{R+} &= \sin \alpha t'_R + \cos \alpha T'_{R+}, \end{aligned} \quad (6)$$

where the mixing angles α and β can be defined by the dimensionless ratio $R = \lambda_1/\lambda_2$ as,

$$\sin \alpha = \frac{R}{\sqrt{1+R^2}}, \quad \sin \beta = \frac{R^2}{1+R^2} \frac{v}{f}. \quad (7)$$

The $t \equiv (t_L, t_R)$ quark is identified with the SM top quark, and $T_+ \equiv (T_{L+}, T_{R+})$ is its T-even heavy partner, which is responsible for the cancelation of the quadratic divergence to the Higgs mass induced by the top quark. The heavy quark T_+ mix with the SM top quark and leads to a modification of the top quark couplings with respect to the SM. Then, the masses of the top quark and its partners up to $\mathcal{O}(v^2/f^2)$ are given by

$$\begin{aligned} m_t &= \frac{\lambda_2 v R}{\sqrt{1+R^2}} \left[1 + \frac{v^2}{f^2} \left(-\frac{1}{3} + \frac{1}{2} \frac{R^2}{(1+R^2)^2} \right) \right] \\ m_{T_+} &= \frac{f m_t (1+R^2)}{v R} \left[1 + \frac{v^2}{f^2} \left(\frac{1}{3} - \frac{R^2}{(1+R^2)^2} \right) \right] \\ m_{T_-} &= \frac{f m_t \sqrt{1+R^2}}{v R} \left[1 + \frac{v^2}{f^2} \left(\frac{1}{3} - \frac{1}{2} \frac{R^2}{(1+R^2)^2} \right) \right] \end{aligned} \quad (8)$$

The T-invariant Lagrangians of the Yukawa interactions of the down-type quarks and charged leptons can be constructed by two possible ways, which are denoted as case A and case B, respectively[8]. In the two cases, the corrections to the Higgs couplings with the down-type quarks and charged leptons with respect to their SM values are given at order $\mathcal{O}(v_{SM}^4/f^4)$ by ($d \equiv d, s, b, \ell_i^\pm$)

$$\begin{aligned} \frac{g_{h\bar{d}d}}{g_{h\bar{d}d}^{SM}} &= 1 - \frac{1}{4} \frac{v_{SM}^2}{f^2} + \frac{7}{32} \frac{v_{SM}^4}{f^4} & \text{case A} \\ \frac{g_{h\bar{d}d}}{g_{h\bar{d}d}^{SM}} &= 1 - \frac{5}{4} \frac{v_{SM}^2}{f^2} - \frac{17}{32} \frac{v_{SM}^4}{f^4} & \text{case B} \end{aligned} \quad (9)$$

III. NUMERICAL RESULTS AND DISCUSSIONS

In the LHT model, the tree-level Feynman diagrams of the process $pp \rightarrow thj$ are shown in Fig.1, where the Higgs is emitted mainly either from a top quark leg or a W boson propagator. Due to the couplings of the Higgs to the W and the top quark have opposite sign, these two diagrams suffer from destructive interference. The T-even top partner T_+ contributes this process through Fig.1(c), which will reflect the LHT effect.

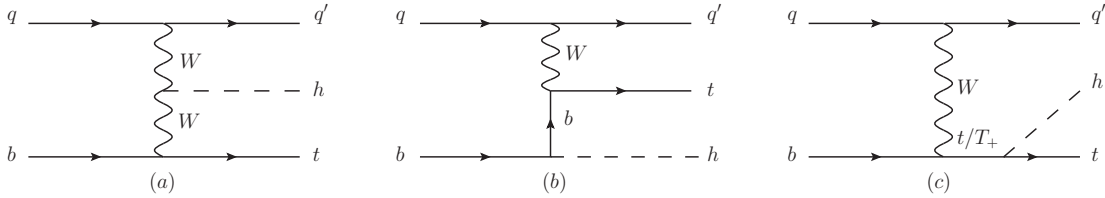


FIG. 1: Feynman diagrams for $pp \rightarrow thj$ in the LHT model at tree level.

In order to investigate the observability, we will perform the Monte Carlo simulation and explore the sensitivity of $pp \rightarrow thj$ at 14 TeV LHC through the channel

$$pp \rightarrow t(\rightarrow \ell^+ \nu b)h(\rightarrow \gamma\gamma)j \quad (10)$$

where j denotes the light jets and $\ell = e, \mu$. At tree level, the signal has three particles (a top quark, a Higgs boson and a forward quark jet) in the final state, which is characterized by appearing as a narrow resonance centered around the Higgs mass. Since the contribution from Fig.1(b) is negligible, the difference for the case A and case B in this signal will mainly come from the branching ratio of $h \rightarrow \gamma\gamma$. We employ the effective Higgs-photon-photon

coupling [9] and calculate the branching ratio of $h \rightarrow \gamma\gamma$ by using the package **HiggsSignals-1.4.0**[10]. We show the ratios $\text{Br}(h \rightarrow \gamma\gamma)_{\text{LHT}}/\text{Br}(h \rightarrow \gamma\gamma)_{\text{SM}}$ as a function of the scale f for two cases in Fig.2. We can see that the $\text{Br}(h \rightarrow \gamma\gamma)$ for case B is larger than that for case A, this is because the $hb\bar{b}$ coupling in the LHT-B is suppressed much sizably so that the branching ratio of $h \rightarrow \gamma\gamma$ is enhanced greatly. Besides, the $\text{Br}(h \rightarrow \gamma\gamma)$ in the LHT model is larger than that in the SM and tends to the SM value with the scale f increasing, which means the LHT effect decouples as the scale f increasing.

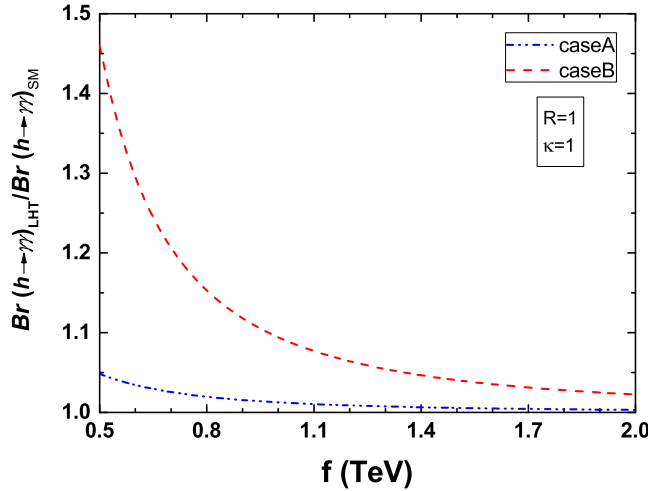


FIG. 2: The ratios $\text{Br}(h \rightarrow \gamma\gamma)_{\text{LHT}}/\text{Br}(h \rightarrow \gamma\gamma)_{\text{SM}}$ versus the scale f for two cases.

The backgrounds can be divided into two classes according to their resonant or nonresonant behavior in the diphoton system:

- (i) resonant backgrounds, including $Whjj$, $Zhjj$ and $t\bar{t}h$, these processes have a Higgs boson decaying to two photons in the final states;
- (ii) nonresonant backgrounds, including $t\bar{t}\gamma\gamma$, $tj\gamma\gamma$ and $Wjj\gamma\gamma$, where the $Wjj\gamma\gamma$ production can mimic the signal when one light jet is mistagged as a b jet.

In our analysis, the backgrounds $Whjj$ and $Zhjj$ are ignored due to their small production cross sections. We generate the signal and background events at the parton level by **MadGraph5**[11], where the $t\bar{t}h$ and $t\bar{t}\gamma\gamma$ events are selected in the single-lepton channel of $t\bar{t}$ decay. The **NNPDF23LO1**[12] parton distribution functions are chosen for our calculations. We set the renormalization scale μ_R and factorization scale μ_F of the signal process to be $\mu_R = \mu_F = (m_t + m_h)/2$, which can be set analogously in the background processes. The

relevant SM input parameters are taken as follows [13]:

$$\begin{aligned} m_t &= 173.07 \text{ GeV}, \quad m_Z = 91.1876 \text{ GeV}, \quad m_h = 125 \text{ GeV}, \\ \sin^2 \theta_W &= 0.231, \quad \alpha(m_Z) = 1/128, \quad \alpha_s(m_Z) = 0.1184. \end{aligned} \quad (11)$$

We feed the events into **Pythia** [14] for parton showering and hadronization. Then, we perform a fast detector simulations by **Delphes** [15], where the (mis)tagging efficiencies are taken as the default values. The subsequent simulations are performed by **MadAnalysis 5** [16]. We chose the basic cuts as follows:

$$\begin{aligned} \Delta R_{ij} &> 0.4, \quad i, j = \gamma, \ell, b \text{ or } j \\ p_T^\gamma &> 10 \text{ GeV}, \quad |\eta_\gamma| < 2.5 \\ p_T^\ell &> 10 \text{ GeV}, \quad |\eta_\ell| < 2.5 \\ p_T^b &> 20 \text{ GeV}, \quad |\eta_b| < 2.5 \\ p_T^j &> 20 \text{ GeV}, \quad |\eta_j| < 5. \end{aligned} \quad (12)$$

In order to reduce the backgrounds and enhance the signal, some additional cuts of kinematic distributions are needed. In Fig.3, we display the normalised transverse momentum distributions $p_T^{\gamma_1}, p_T^{\gamma_2}$ of two photons, the normalised invariant mass distribution $M_{\gamma_1\gamma_2}$ of two photons, the normalised transverse mass distribution $M_T(\gamma_1\gamma_2 b_1 l_1^+)$ of the $\gamma_1\gamma_2 b_1 l_1^+ \cancel{E}_T$ system in the signal and backgrounds at 14 TeV LHC for $R = 1$, where the transverse mass M_T is defined as

$$M_T^2 \equiv \left(\sqrt{(p_\ell + p_b)^2 + |\vec{p}_{T,\ell} + \vec{p}_{T,b}|^2} + |\vec{p}_T| \right)^2 - |\vec{p}_{T,\ell} + \vec{p}_{T,b} + \vec{p}_T|^2, \quad (13)$$

where $\vec{p}_{T,\ell}$ and $\vec{p}_{T,b}$ are respectively the transverse momentums of the charged leptons and b -quark, and \vec{p}_T is the missing transverse momentum derived from the negative sum of visible momenta in the transverse direction.

Since the two photons in the signal and the resonant backgrounds come from the Higgs boson, they have the harder p_T spectrum than those in the non-resonant backgrounds. Thus, we can apply the cuts of two photons to suppress the non-resonant backgrounds. Next, the signal and the resonant backgrounds have the diphoton invariant-mass peak at m_h , which can be used to further reduce the non-resonant backgrounds. Besides, due to the resonance effect of the top partner T_+ , the transverse mass distribution $M_T(\gamma_1\gamma_2 b_1 l_1^+)$ have endpoints round m_{T_+} in the signal, which can be used to remove the backgrounds effectively.

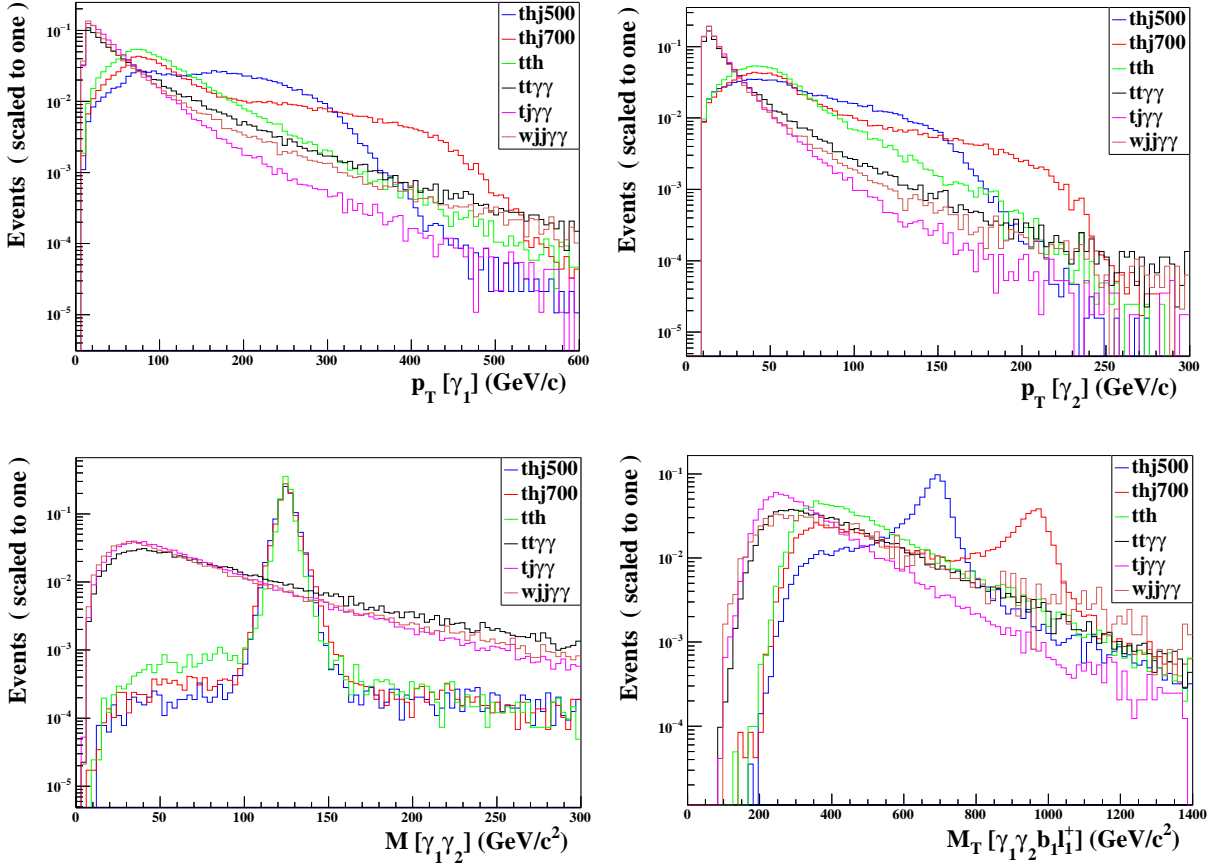


FIG. 3: The normalised distributions of $p_T^{\gamma_1}, p_T^{\gamma_2}, M_{\gamma_1 \gamma_2}, M_{\gamma_1 \gamma_2 b_1 l_1^+}$ after the basic cuts in the signal and backgrounds at 14 TeV LHC for $R = 1$.

According to the above analysis, we require the events after the basic cuts to satisfy the following criteria:

$$\text{Cut-1 : } p_T^{\gamma_1} > 60\text{GeV}, p_T^{\gamma_2} > 30\text{GeV};$$

$$\text{Cut-2 : } |M_{\gamma\gamma} - m_h| < 10\text{GeV};$$

$$\text{Cut-3 : } M_{\gamma_1 \gamma_2 b_1 l_1^+} > 550\text{GeV}.$$

In Table.I, we summarize the cut-flow cross sections of the signal and backgrounds after imposing the cuts. For comparison, we chose two sets of benchmark points that ($f = 500$ GeV, $R = 1$) correspond to $m_{T_+} = 702$ GeV and ($f = 700$ GeV, $R = 1$) correspond to $m_{T_+} = 984$ GeV, which satisfy the constraint of the current Higgs data and the electroweak precision observables(EWPO)[17]. As we know, the process $pp \rightarrow thj$ exists in the SM. The leading-order cross section for this process is $\sigma_{\text{SM}}^{14\text{TeV}}(pp \rightarrow thj) = 80.4$ fb[18], which retains about 0.02 fb after the subsequent decays and the basic cuts.

TABLE I: Cutflow of the cross sections for the signal and backgrounds at 14 TeV LHC on the benchmark points ($f = 500$ GeV, $R = 1$) and ($f = 700$ GeV, $R = 1$) for two cases. All the conjugate processes of the signal and backgrounds have been included.

Cuts	$\sigma(\times 10^{-3}\text{fb})$							
	Signal-caseA		Signal-caseB		Backgrounds			
	$thj500$	$thj700$	$thj500$	$thj700$	$t\bar{t}h$	$t\bar{t}\gamma\gamma$	$tj\gamma\gamma$	$Wjj\gamma\gamma$
Basic cuts	65.7	33.7	91.5	39.8	204	4462	3091	35770
$p_T^{\gamma_1} > 60\text{GeV}$ $p_T^{\gamma_2} > 30\text{GeV}$	34.6	15.9	48.2	18.8	71.5	665.8	411.1	4494
$ M_{\gamma\gamma} - m_h < 10\text{GeV}$	29.8	13.7	41.5	16.2	66.1	65.9	45.2	449.4
$M_{\gamma_1\gamma_2 b_1 l_1^+} > 550\text{GeV}$	10.3	3.3	14.3	3.9	9.9	8.6	4.0	8.5

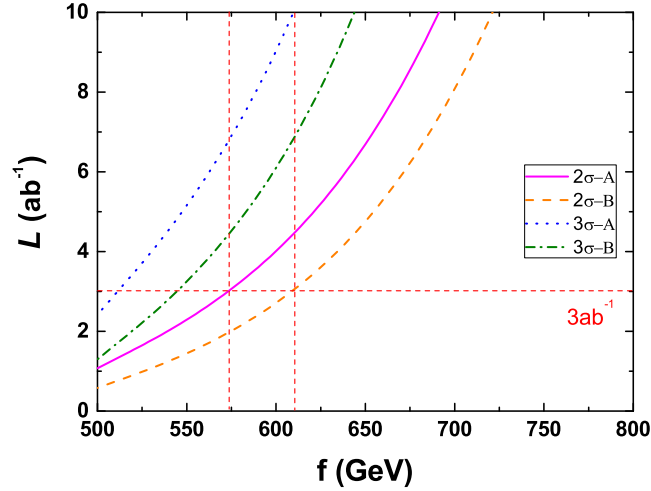


FIG. 4: The statistical significance of $pp \rightarrow t(\rightarrow \ell^+ \nu b)h(\rightarrow \gamma\gamma)j$ at 14 TeV LHC on the $L \sim f$ plane for $R = 1$ in two cases. The contribution of the charge conjugate process has been included.

To estimate the observability quantitatively, the Statistical Significance (SS) is calculated after final cut by using Poisson formula[19]

$$SS = \sqrt{2L \left[(S + B) \ln \left(1 + \frac{S}{B} \right) - S \right]}, \quad (14)$$

where S and B are the signal and background cross sections and L is the integrated luminosity. The results of the SS values depending on the integrated luminosity L at 14TeV LHC for $R = 1$ in two cases are shown in Fig.4, where the contours of 2σ and 3σ significance

are displayed. We can see that the scale f can be excluded up to 573 GeV (correspond to $m_{T_+}=805$ GeV) for case A and 610 GeV (correspond to $m_{T_+}=857$ GeV) for case B at 2σ confidence level at 14 TeV LHC with the integrated luminosity $L = 3\text{ab}^{-1}$. If the integrated luminosity can reach 10ab^{-1} , the 2σ exclusion limit of the scale f will be pushed up to 690 GeV (correspond to $m_{T_+}=970$ GeV) for case A and 720 GeV (correspond to $m_{T_+}=1012$ GeV) for case B.

For the process $pp \rightarrow thj$, comparing the result of decay $h \rightarrow \gamma\gamma$ with that of decay $h \rightarrow b\bar{b}$ in Ref.[7], we can see that the limits on the T_+ mass from $h \rightarrow \gamma\gamma$ are weaker than that from $h \rightarrow b\bar{b}$. For the result of decay $h \rightarrow b\bar{b}$, it is worth noting that the limit on m_{T_+} for case B is lower than that for case A, which is because the smaller bottom Yukawa coupling in case B (cf. Eq.(9)) leads to a higher suppression of the branching ratio of $h \rightarrow b\bar{b}$. By contrast, the branching ratio of $h \rightarrow \gamma\gamma$ for case B is larger than that for case A as shown in Fig.2. As a result, the limits on m_{T_+} from the thj production with $h \rightarrow \gamma\gamma$ for the two cases are just the reverse.

Besides, the limits on the T_+ mass from the global fit of the Higgs data and EWPO have been performed in Ref.[17], where the T_+ mass can be excluded up to 920(750) GeV for case A(B). Combining the case A and case B, we can see that the limits on the T_+ mass from the thj production with $h \rightarrow \gamma\gamma$ at LHC with High-Luminosity can be comparable with the global fit of the Higgs data and EWPO.

Recently, the direct searches for the vector-like T at 13 TeV LHC have been performed by ATLAS[20] and CMS[21] Collaborations relying on signatures induced by both the vector-like T pair-production and single-production modes, corresponding to an integrated luminosity of about 36fb^{-1} . For the pure Wb decay, the observed (expected) 95% CL lower limits on the T mass are 1350 GeV (1310GeV). For the pure Zt decay, the observed (expected) 95% CL lower limits on the T mass are 1160 GeV (1170 GeV). However, their bounds strongly depend on the assumptions on the decay branching ratios and the properties of the top partner, especially its group representations. In the LHT model, these limits can be relaxed due to the impure decay modes of the top partner T_+ and the specific group representations, and the detailed confirmation will require the Monte Carlo simulations of the signals and backgrounds and the comprehensive collider analysis.

IV. SUMMARY

In the framework of the LHT model, we investigate the observability of $pp \rightarrow thj$ with decays $t \rightarrow \ell^+ \nu b$ and $h \rightarrow \gamma\gamma$ at 14 TeV LHC. By performing a fast detector simulation, we find that the thj search in the selected channel can excluded the m_{T_+} up to 805 GeV for case A and 857 GeV for case B at 2σ confidence level at 14 TeV LHC with the integrated luminosity $L = 3\text{ab}^{-1}$. This excluded region will be further expanded if the higher integrated luminosity is obtained at the LHC.

Acknowledgement

This work was supported by the National Natural Science Foundation of China (NNSFC) under grants No.11405047 and the Startup Foundation for Doctors of Henan Normal University under Grant No.qd15207.

-
- [1] G. Aad et al. [ATLAS Collaboration], Phys. Lett. B 716 (2012) 1; S. Chatrchyan et al. [CMS Collaboration], Phys. Lett. B 716 (2012) 30.
 - [2] see examples: C. C. Han, N. Liu, L. Wu, J. M. Yang, Phys. Lett. B 714 (2012) 295-300; J. Cao, L. Wang, L. Wu, J. M. Yang, Phys. Rev. D 84 (2011) 074001; B. F. Yang, X. D. Li, Commun. Theor. Phys. 59 (2013) 87-94.
 - [3] G. Bordes and B. van Eijk, Phys. Lett. B 299 (1993) 315; A. Ballestrero and E. Maina, Phys. Lett. B 299 (1993) 312; W. J. Stirling and D. J. Summers, Phys. Lett. B 283 (1992) 411; J. L. Diaz-Cruz and O. A. Sampayo, Phys. Lett. B 276 (1992) 211.
 - [4] V. Khachatryan et al. [CMS Collaboration], CMS PAS HIG-14-001, CMS PAS HIG-14-015, CMS PAS HIG-14-026, JHEP 1606 (2016) 177.
 - [5] see recent examples: L. Wu, JHEP 02 (2015) 061; A. Kobakhidze, L. Wu, J. Yue, JHEP 10 (2014) 100; P. Agrawal, S. Mitra, A. Shivaji, JHEP 12 (2013) 077; S. Biswas, E. Gabrielli, B. Mele, JHEP 01 (2013) 088; S. Biswas, E. Gabrielli, F. Margaroli, B. Mele, JHEP 07 (2013) 073; B. F. Yang, Z. Y. Liu, J. Z. Han and G. Yang, Adv. High Energy Phys. 2016 (2016) 2613187; Y. M. Zhang and B. F. Yang, EPL 110 (2015) 21001; G. R. Lu and L. Wu, Chin. Phys. Lett. 27 (2010) 031401; J. Chang, K. Cheung, J. S. Lee, and C.-T. Lu, JHEP 1405

- (2014) 062; F. Demartin, F. Maltoni, K. Mawatari, and M. Zaro, Eur. Phys. J. C 75 (2015) 267.
- [6] H. C. Cheng and I. Low, JHEP 0309 (2003) 051; JHEP 0408 (2004) 061; I. Low, JHEP 0410 (2004) 067; J. Hubisz and P. Meade, Phys. Rev. D 71 (2005) 035016.
- [7] B. F. Yang, J. Z. Han and N. Liu, JHEP 04 (2015) 148.
- [8] C. R. Chen, K. Tobe, C. P. Yuan, Phys. Lett. B 640 (2006) 263.
- [9] T. Han, H. E. Logan, B. McElrath, L.-T. Wang, Phys. Lett. B 563 (2003) 191; J. F. Gunion, H.E. Haber, G.L. Kane, and S. Dawson, The Higgs Hunters Guide, Addison-Wesley, Reading, MA, U.S.A. (1990).
- [10] P. Bechtle, S. Heinemeyer, O. Stål, T. Stefaniak and G. Weiglein, Eur. Phys. J. C 74 (2014) 2711; P. Bechtle, O. Brein, S. Heinemeyer, G. Weiglein and K.E. Williams, Comput. Phys. Commun. 181 (2010) 138.
- [11] J. Alwall, M. Herquet, F. Maltoni, O. Mattelaer and T. Stelzer, JHEP 06 (2011) 128.
- [12] R. D. Ball et al. [NNPDF Collaboration], Nucl. Phys. B 877 (2013) 290.
- [13] C. Patrignani et al., (Particle Data Group), Chin. Phys. C 40(10) (2016) 100001.
- [14] T. Sjostrand, S. Mrenna and P. Z. Skands, JHEP 0605 (2006) 026.
- [15] J. de Favereau, et al., JHEP 1402 (2014) 057.
- [16] E. Conte, B. Fuks, G. Serret, Comput. Phys. Commun. 184 (2013) 222-256.
- [17] J. Reuter, M. Tonini, M. de Vries, JHEP 1402 (2014) 053; B. F. Yang, G. F. Mi, N. Liu, JHEP 10 (2014) 047; B. F. Yang, J. Z. Han and N. Liu, Phys. Rev. D 95 (2017) 035010; C. C. Han, A. Kobakhidze, N. Liu, L. Wu, B. F. Yang, Nucl. Phys. B 890(2015)388-399; N. Liu, L. Wu, B. F. Yang, M. C. Zhang, Phys. Lett. B 753 (2016) 664-669; H. Y. Wang and B. F. Yang, Adv. High Energy Phys. 2017 (2017) 5463128.
- [18] M. Farina, C. Grojean, F. Maltoni, E. Salvioni and A. Thamm, JHEP 05 (2013) 022.
- [19] G. Cowan, K. Cranmer, E. Gross, and O. Vitells, Eur. Phys. J. C 71 (2011) 1554.
- [20] ATLAS Collaboration, JHEP 10 (2017) 141, JHEP 08 (2017) 052.
- [21] CMS Collaboration, CMS-B2G-17-003, CMS-B2G-17-007.